Theory of spin-density profile and lattice distortion in the magnetization plateaus of $SrCu_2(BO_3)_2$

Shin Miyahara,[1] Federico Becca,[1,2] and Frédéric Mila[1]
[1]*Institut de Physique Théorique, Université de Lausanne, CH-1015 Lausanne, Switzerland*
[2]*INFM-Democritos, National Simulation Centre, and SISSA I-34014 Trieste, Italy*
(Received 11 December 2002; published 2 July 2003)

The two-dimensional spin-gap system $SrCu_2(BO_3)_2$ shows unique physical properties due to the low-dimensionality character and the strong quantum fluctuations. Experimentally, 1/8, 1/4, and 1/3 plateaus have been observed in the magnetization curve under magnetic fields up to 70 T, and the 1/2 plateau is expected to be stabilized at higher magnetic fields. We argue that spin-lattice effects are necessary to describe the spin density profile at the plateaus, and we propose a simple microscopic model of spins interacting adiabatically with the lattice to reproduce the main features of the recent experimental results by nuclear magnetic resonance.

DOI: 10.1103/PhysRevB.68.024401 PACS number(s): 75.10.Jm, 75.30.Kz

I. INTRODUCTION

The possibility to obtain low-dimensional quantum spin systems that do not order magnetically at very low temperature, or even down to zero temperature, is currently a subject of great interest. Although there are many examples of one-dimensional (1D) or quasi-1D systems such as $SrCu_2O_3$ ($S=1/2$ ladder),[1] Y_2BaNiO_5 (Haldane chain),[2] $CuGeO_3$ and LiV_2O_5 (prototype of frustrated $S=1/2$ chains),[3,4] for some time, the only example of a two-dimensional (2D) system with a singlet ground state and a finite gap to magnetic excitations was the vanadium oxide CaV_4O_9 (Refs. 5–7). Therefore, the recent discovery of $SrCu_2(BO_3)_2$ (Ref. 8) represents a breakthrough in this direction, and paves the way for further research on this unconventional state of matter. This compound has a layered structure where stacking layers of $CuBO_3$ are intercalated by magnetically inert layers of Sr. A spin $S=1/2$ resides on each Cu^{2+} ion, forming a 2D orthogonal dimer lattice[8] (see Fig. 1). It turns out that the magnetic properties of $SrCu_2(BO_3)_2$ are very well described by the 2D orthogonal dimer Heisenberg model,[9,10] which is topologically equivalent to the 2D Shastry-Sutherland model:[11]

$$\mathcal{H}=J\sum_{\text{(n.n.)}}\mathbf{S}_i\cdot\mathbf{S}_j+J'\sum_{\text{(n.n.n.)}}\mathbf{S}_i\cdot\mathbf{S}_j; \tag{1}$$

here $\mathbf{S}_i=(S_i^x,S_i^y,S_i^z)$ is the spin-1/2 operator at the site i and the notations (n.n.) and (n.n.n.) stand for nearest-neighbor and next-nearest-neighbor sites, respectively. In the parameter range $J'/J<0.68$ (Ref. 12) the ground state is exactly known to be the product of dimer singlets:[11]

$$|\Psi\rangle=\prod_a\frac{1}{\sqrt{2}}(|\uparrow\downarrow\rangle_a-|\downarrow\uparrow\rangle_a), \tag{2}$$

where a indicates the dimer bond connected by the superexchange coupling J. In Ref. 13, it was shown that the values of the antiferromagnetic superexchange are such that $J'/J=0.635$, with $J=85$ K, indicating that $SrCu_2(BO_3)_2$ can be described by a 2D spin system whose ground state is exactly known.

The very particular nature of the ground state induces unique features in the spin excitations at low temperatures. First of all, there is a finite gap to the magnetic excitations. This spin gap has been observed in several experiments and was estimated to be about 35 K.[14–17] Moreover, the triplet excitations have an almost localized nature because of the orthogonality of the J bonds.[9] Such a behavior was revealed experimentally, using inelastic neutron scattering,[15] as an almost flat triplet dispersion.

The localized nature of the triplet excitation leads also to the most spectacular phenomenon of this system: When an external magnetic field, up to 70 T, is applied, the system shows magnetization plateaus corresponding to 1/8, 1/4, and 1/3 of the full Cu^{2+} moment (another plateau at 1/2 of the full Cu^{2+} moment is likely to be stabilized at even higher magnetic fields).[8,18] By applying an external magnetic field, the density of the triplets can be tuned and it is found that the magnetization stays constant for particular ranges of the external field. It is expected that the plateaus are due to a crys-

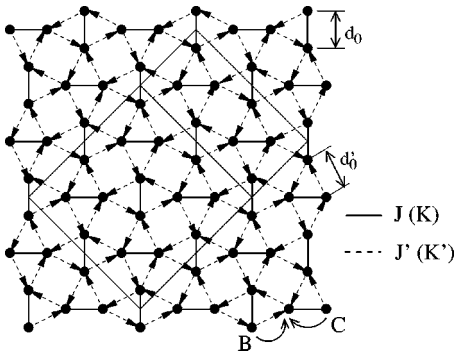

FIG. 1. The orthogonal dimer lattice. The continuous and dashed lines indicate the antiferromagnetic interactions and the elastic couplings for nearest neighbor and next-nearest neighbor sites, respectively. The nearest neighbor and the next-nearest neighbor equilibrium distances are indicated by d_0 and d_0', respectively. The 16-site square cluster and 24-site rectangular cluster used in the calculations are shown by thin solid lines. The transferred hyperfine couplings B and C (see Sec. IV) are also shown. The arrows define the direction from the site i to the site j for the Dzyaloshinsky-Moriya interaction (see Sec. IV B).

tallization of the triplets for particular commensurate values of the magnetization and are due to the small ratio between the kinetic and the interaction energy of the triplets. To our knowledge, $SrCu_2(BO_3)_2$ is the first example of a 2D quantum spin system which shows magnetization plateaus.

So far, the magnetization plateaus have been studied mostly in 1D systems.[19–22] In particular, Yamanaka, Oshikawa, and Affleck[23] have found a simple necessary condition for the existence of plateaus in 1D systems. Denoting by l the period of the ground state in the presence of the external field, by S the magnitude of the spin, and by m the magnetization per site (in units of $g\mu_B$), the occurrence of a magnetization plateau is only possible when the condition

$$l(S-m)=\text{integer}, \tag{3}$$

is satisfied. It is important to mention that l can be different from the period of the lattice. The first example of a magnetization plateau accompanied by such a symmetry breaking is a $S=1/2$ Heisenberg chain with next-nearest-neighbor and alternating nearest-neighbor interactions.[24,25]

Recently, Oshikawa extended the Lieb-Schultz-Mattis argument to quantum many-particle systems with a conserved particle number on a periodic lattice in arbitrary dimensions and showed that the condition of Eq. (3) for the plateau is still valid in arbitrary dimensions.[26] Indeed, several theoretical works concerning the plateaus for $SrCu_2(BO_3)_2$ indicate that the criterion of Eq. (3) is satisfied and, except for the plateau at 1/2, the ground states at the plateaus are accompanied by a breaking of the translational symmetry.[27–32]

Recently, Kodama and collaborators[33] performed a nuclear magnetic resonance (NMR) measurement at the 1/8 plateau, for an external magnetic field $H=27.6$ T and a temperature of 35 mK, and observed the presence of at least 11 *different* sites (i.e., different values of the local magnetization), indicating a clear breaking of the translational symmetry. So far, from a theoretical point of view, the superstructures at the plateaus have been studied only by an effective hard-core boson model. In this approximation, the triplet with $S^z=1$ is represented by a hard-core boson and the dimer singlet by a vacancy. An effective Hamiltonian is derived by perturbation theory and the magnetization curve and superstructures have been calculated by solving it.[27–31] In this picture, two different unit cells with 16 sites have been proposed to describe this plateau:(i) a 16-site square unit cell, and (ii) a rhomboid unit cell.[29] However, the ground state at the 1/8 plateau is described by a state where one of the eight singlets is promoted to a triplet within the unit cell. Thus there are only two different sites, corresponding to the singlet and the triplet states, and it cannot reproduce the very rich texture of the magnetization observed in NMR experiments. Therefore, in order to reproduce the experimental data, the simple hard-core boson model is not sufficient and it is necessary to consider the original spin Hamiltonian.

From the results of the hard-core boson calculations, as well as from the result of Ref. 26, it is expected that the translational symmetry is broken inside the plateaux, and that the ground state is degenerate, except for the 1/2 plateau. However, a local quantity such as magnetization $\langle S_i^z\rangle$, which is directly accessible in NMR, will only be observed if an extra mechanism selects one of the ground states, since linear combinations of the ground states can lead to an *arbitrary* magnetization even if the translational symmetry is broken. For instance, a uniform linear combination would lead to a uniform magnetization. In the real material, this mechanism could *a priori* be due to pinning by impurities, or to a lattice distortion. Actually, a strong motivation for considering lattice effects in $SrCu_2(BO_3)_2$ is given by the pronounced softening of the sound velocity observed at the edges of the magnetization plateau.[34,35] On the theoretical side, one could try to select a magnetization texture by imposing an external, very small symmetry breaking field, as is often done for instance for the dimerized state in a spin-Peierls system. However, in the present case, we do not know *a priori* the magnetization texture, and imposing a specific field would bias the results. Therefore, we prefer the more physical way which consists in coupling the system to phonons.

The paper is organized as follows. In Sec. II, we introduce the spin-phonon Hamiltonian and explain the method. In Sec. III, we present the results for the superstructures at 1/8, 1/4, 1/3, and 1/2 plateaus. In Sec. IV we compare our theoretical results for the 1/8 plateau to the experimental ones, including in addition the effects of interlayer coupling and Dzyaloshinsky-Moriya interaction. Finally, Sec. V is devoted to the conclusions and the discussion.

II. MODEL AND METHOD

In this section we introduce the spin-phonon Hamiltonian and we describe the method that we use to characterize the spin texture of the different magnetization plateaus. We consider the $S=1/2$ orthogonal dimer model coupled to adiabatic phonons that we study by exact diagonalizations of finite clusters with a self-consistent Lanczos algorithm. In this approach, the adiabatic phonons are described by classical variables, related to the displacements of the lattice sites. The full spin-phonon Hamiltonian is defined on a 2D orthogonal dimer lattice of N sites by

$$\mathcal{H}=\sum_{(\text{n.n.})}\left\{J(d_{ij})\mathbf{S}_i\cdot\mathbf{S}_j+\frac{K}{2}\left(\frac{\|\delta\mathbf{r}_i-\delta\mathbf{r}_j\|}{d_{ij}^0}\right)^2\right\}$$
$$+\sum_{(\text{n.n.n.})}\left\{J'(d_{ij})\mathbf{S}_i\cdot\mathbf{S}_j+\frac{K'}{2}\left(\frac{\|\delta\mathbf{r}_i-\delta\mathbf{r}_j\|}{d_{ij}^0}\right)^2\right\}; \tag{4}$$

here $J(d_{ij})$ and $J'(d_{ij})$ are the antiferromagnetic superexchange couplings, which depend on the relative distance $d_{ij}=\|\mathbf{R}_i^0+\delta\mathbf{r}_i-\mathbf{R}_j^0-\delta\mathbf{r}_j\|$ between sites i and j. K and K' are the elastic coupling constants, $\delta d_{ij}=d_{ij}-d_{ij}^0$, and $d_{ij}^0=\|\mathbf{R}_i^0-\mathbf{R}_j^0\|$ is the equilibrium distances between Copper sites.

For small displacements of the Cu sites, it is possible to linearize the antiferromagnetic couplings around their equilibrium values, $\delta d_{ij}\simeq(\mathbf{R}_i^0-\mathbf{R}_j^0)\cdot(\delta\mathbf{r}_i-\delta\mathbf{r}_j)$, and therefore we expect that in general:[36]

$$J(d_{ij})=J\left(\frac{d_{ij}^0}{d_{ij}}\right)^{\alpha}\simeq J\left(1-\alpha\frac{\delta d_{ij}}{d_{ij}^0}\right). \tag{5}$$

In the following, we will denote by α and α' the two (in principle different) exponents for $J(d_{ij})$ and $J'(d_{ij})$, respectively.

With a self-consistent Lanczos diagonalization of finite clusters, one can find the optimal configuration of the bond lengths and local spin configurations for given values of the coupling parameters (α, α', K and K') and given total spin S quite easily: Starting from a random choice of the atomic displacements, one just has to improve iteratively the total energy by changing the lattice parameters until a stationary configuration is reached. In all cases, we have verified that this configuration is stable and unique (up to trivial symmetry operations) by starting from different initial distributions, so it must be the global minimum. This method has been already used for other 1D, quasi-1D, and 2D spin systems interacting adiabatically with the lattice.[37,38] With respect to other approximate approaches, this method has the great advantage that it gives unbiased results even for strongly frustrated systems, where other numerical methods can be highly questionable. It is worth noting that, in our self-consistent Lanczos method, the only approximation is to consider the adiabatic limit for the phonons. Once we restrict our calculation to this case, we obtain exact results for the lattice distortions on the chosen finite cluster.

In the following, we consider unit cells containing $N=16$ sites or, in some case, up to $N=24$ sites with periodic boundary conditions (see Fig. 1). In our simple microscopic model, we assume that the magnetic field directly couples to the total spin of the system, stabilizing the states with higher total spin. Because of the finiteness of our cluster, in order to study the plateau at $1/n$, we assume that the external field is able to stabilize a state with a given magnetization and we fix the total spin of the cluster (by fixing $S^z_{tot}=\Sigma_i S^z_i = N/2n$). It is worth mentioning that, within our self-consistent Lanczos method, we are not able to study the actual width of the magnetization plateau in the thermodynamic limit. Nonetheless, once the existence of a given plateau is assumed, we can produce important insight into the local structure of the spins inside the cell.

In the following calculations, we consider the case of $\alpha'=1.75\alpha$ and $K=K'=750J'$, but we want to stress that all the results are not specific of this particular choice and, qualitatively, we found similar results also for different values of these parameters. The parameters K and K' are only effective parameters that cannot be directly matched to the phonon dispersion. An appropriate model of elastic constants should include the springs between all nearest neighbor atoms, but this does not improve the calculation because the dependence of the spring constants on the actual position of all atoms is not exactly known. Nevertheless, the order of magnitude of the elastic constants is expected to be similar in all oxides. For instance, for $CuGeO_3$, in order to have relative displacements smaller than a percent — as observed experimentally in the spin-Peierls phase – the values of the elastic constants are required to be of the order of 100000 K.[39] Finally, superexchange theory suggests that typical value for α in oxides are in the range 6-14 (Ref. 36).

The bond length of nearest neighbor bond d_0 is taken as the unit of the length, which is 2.91 Å at 100 K, and the length of next-nearest neighbor bond d_0' is assumed to be given by $d_0'=1.75d_0$ (Ref. 40). Finally, we note that Hamiltonian (4) is invariant under the rescaling $\alpha\rightarrow\lambda\alpha$, $\alpha'\rightarrow\lambda\alpha'$, $K\rightarrow\lambda^2K$, $K'\rightarrow\lambda^2K'$, and $\delta\mathbf{r}_i\rightarrow\delta\mathbf{r}_i/\lambda$, where λ is the rescaling parameter. This allows us to fix one parameter among α, α', K and K'. Note that the physical values of the magnetic couplings are unaffected by this transformation.

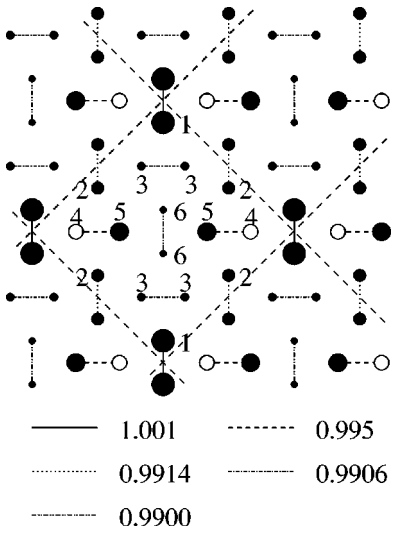

FIG. 2. Spin density profile for the 1/8 plateau for the 16-site square cluster. Full (empty) circles indicate sites with magnetization along (opposite to) the external field and the size of the circles is proportional to the spin amplitude. The bond lengths for $\alpha=10$ are also shown.

III. EFFECT OF SPIN-PHONON COUPLING AT PLATEAUS

A. 1/8 plateau

In order to describe the two most probable triplet patterns that were previously suggested for the 1/8-plateau by the hard-core boson approach,[29] we have diagonalized Hamiltonian (4) on two 16-site clusters corresponding to different unit cells, the 16-site square cluster and the rhomboid cluster in the sector with $S^z_{tot}=1$ (see Figs. 2 and 3). The results for the two cases turn out to be qualitatively different: In the square cluster we find that the ground state has only six different sites, that is six different values of the local magnetization $\langle S^z_i\rangle$ (see Fig. 2), whereas the rhomboid cluster contains eight different sites with different local magnetization (see Fig. 3). The energy difference between these two states is very small (of the order of 10^{-5}–10^{-6} J per site). In both cases, the magnetization is centered around one strongly polarized dimer, that, in the following, we will denote by ''triplet,'' with Friedel-like oscillations in the spin amplitude. It is worth noting that we obtain both positive and negative magnetizations, and in particular, in both clusters, there is a large negative spin, just near to the strongly polarized dimer.

One of the main features of these results is the existence of two sites with large and positive polarization and one site with large and negative polarization, which is in agreement with the NMR experimental finding.[33] The Friedel-like oscil-

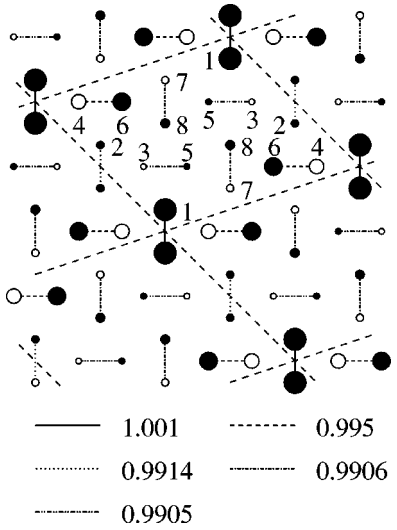

FIG. 3. Spin density profile for the 1/8 plateau for the rhomboid cluster of 16 sites. Full (empty) circles indicate sites with magnetization along (opposite to) the external field and the size of the circles is proportional to the spin amplitude. The bond lengths for $\alpha=10$ are also shown.

lations decay quite fast in space, and far from the ''triplet'' dimer the local magnetization is very small. For this reason, we expect rather small size effects for our finite cluster calculation and we believe that even the 16-site lattice can represent quite well the real system. Of course, we cannot rule out that a larger number of different sites (with very small magnetizations) exists when a bigger cluster is considered, but the very fast decay in the oscillation of the local magnetization clearly indicates that our small 16-site cluster is able to capture the main ingredients of the true ground state: Two sites with large and positive $\langle S_i^z \rangle$, one site with large and negative $\langle S_i^z \rangle$ and a bunch of sites with rather small (positive and negative) magnetizations. Unfortunately, the fact that we do not want to impose any external constraint on the spin pattern prevents us from using the lattice symmetries in the Lanczos diagonalization, and, in order to obtain the optimal lattice (and spin) configuration, it is necessary to perform the diagonalization several times up to convergence. These two facts make the calculation very heavy, and the next cluster, with 32 sites, which is consistent with the 1/8 plateau, is beyond the present computational possibilities.

In the optimized lattice configuration, all the translational symmetries are broken. The ground state is eightfold degenerate for the square unit cell. On the other hand, in the rhomboid case, two types of unit cell are possible and so the ground state is 16 fold degenerate. The behavior of the local magnetization as a function of the spin-phonon coupling is reported in Figs. 4 and 5 for the square and rhomboid clusters, respectively. Notice that below a critical value of the spin-phonon coupling α, a state with a different number of sites is stabilized (four sites for the square cluster and only one for the rhomboid cluster). This is due to the fact that in the 16-site square (rhomboid) cluster without spin-phonon coupling, the ground state is fourfold (twofold) degenerate, and the other low-lying states are separated by a finite-size

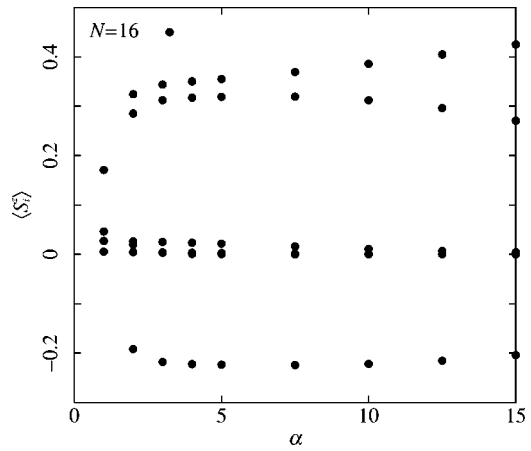

FIG. 4. Local magnetization for the six different sites of the 16-site square cluster for the 1/8 plateau as function of the spin-phonon coupling α.

gap. Thus for a small enough spin-phonon coupling, the ground state corresponds to a linear combination of only four (two) states, and it is only possible to mix all the eight low-lying states with a sufficiently large coupling, resulting in a state with six (eight) different sites. The critical value of the spin-phonon coupling is much larger for the rhomboid cell (of the order of 5) than for the square unit cell (between 1 and 2); see Figs. 4 and 5. As in the spin-Peierls case,[39] it is expected to decrease by enlarging the lattice size; unfortunately, for reasons given just above, it is impossible to attempt a size scaling of this value. For both unit cells, we recover the hard-core boson results of Ref. 29 in the extreme limit of infinite spin-phonon coupling ($\alpha \to \infty$), where all the magnetization is carried by a localized triplet dimer, and all the other dimers are perfect singlets.

Finally, we want to make a remark on the lattice displacements. The magnetic energy gain is related to a shrinking of the bond length of the ''singlets,'' whereas the ''triplet'' dimers enlarge their bond length. The bond lengths for $\alpha = 10$ for square (rhomboid) unit cell are shown in Fig. 2 (Fig. 3). However, for realistic values of the elastic constants and

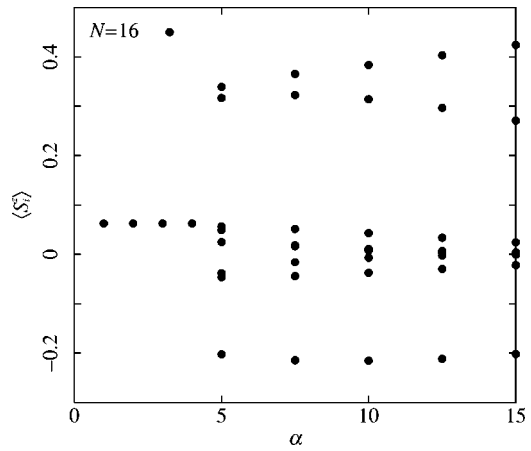

FIG. 5. Local magnetization for the eight different sites of the rhomboid cluster for the 1/8 plateau as a function of the spin-phonon coupling α.

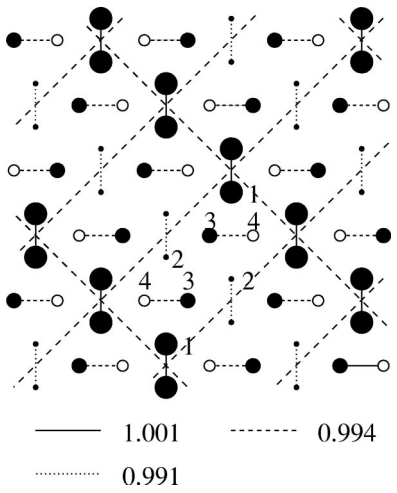

FIG. 6. Spin density profile for the 1/4 plateau. Full (empty) circles indicate sites with magnetization along (opposite to) the external field and the size of the circles is proportional to the spin amplitude. The bond lengths for $\alpha=10$ are also shown.

the spin-phonon coupling, these displacements are very small — of the order of 1 % or less — and we do not think that there is any chance at the moment to detect such a tiny structural distortion with x rays in a field of 27.6 T.

B. 1/4 plateau

Experimentally the next magnetization plateau is at 1/4 of the total Cu^{2+} moment. From the hard-core boson calculations,[29] it comes out that the unit cell is just half of the previous 16-site square cluster. Therefore, for this plateau, we consider the 16-site square lattice and we perform the self-consistent Lanczos method in the sector $S^z_{tot}=2$. Moreover, we also report some results for a larger 24-site rectangular lattice with $S^z_{tot}=3$.

The typical outcome of our exact calculation is shown in Fig. 6: We find four different sites, three with a positive magnetization and one with a negative magnetization. Also in this case, the ''triplet'' dimer is almost localized and the system shows Friedel-like oscillations on the spin amplitude, the nearest site to the ''triplet'' having negative $\langle S^z\rangle$. The ground state is eight-fold degenerate and the eight states are found to be connected by simple symmetry operations of the lattice, like translations and/or reflections. The behavior of the local magnetization as a function of the spin-phonon coupling is reported in Fig. 7 and it clearly indicates that, by increasing α, the total magnetization concentrates progressively in the ''triplet'' dimer and the local magnetizations of the other dimers tend to zero. In the extreme limit of $\alpha\rightarrow\infty$, the picture corresponds to the hard-core boson approximation, where there is only one triplet that carries all the magnetization.[29,31]

Notice that the spin texture is built up by diagonal stripes of strongly polarized dimers, i.e., ''triplets,'' intercalated by dimers with a small polarization. This picture comes out from the fact that there are repulsive interactions between the triplets, which make the stripe structure stable (this can be seen, for example, in the perturbation theory[29,31]).

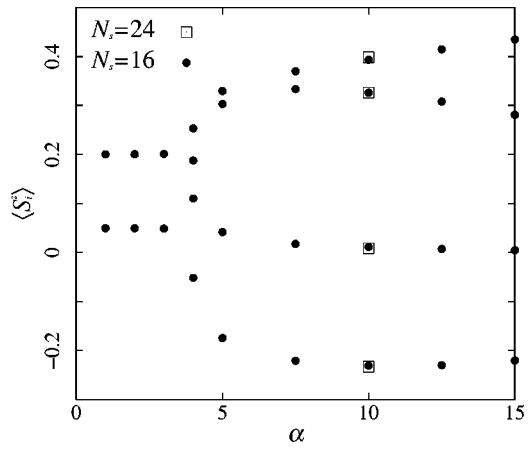

FIG. 7. Local magnetization for four different sites for the 1/4 plateau as a function of the spin-phonon coupling α. The full dots indicate the results for the 16-site cluster and the empty squares the results for the 24-site one at $\alpha=10$.

C. 1/3 plateau

In order to study the 1/3 plateau, we are forced to consider a 24-site cluster with $S^z_{tot}=4$ because in the 16-site cluster the corresponding spin sector is not present. It is worth noting that this cluster breaks the reflection symmetries of the original orthogonal dimer lattice; on the other hand, the shape of this cluster fits well the pattern suggested in previous hard-core boson calculations.[27–30] For this plateau, the Lanczos results display three different values of the local spin (see Fig. 8): A large and positive site, which corresponds to the strongly polarized ''triplet'' dimer, and two small sites (one positive and one negative), building up the other ''singlet'' dimers. The local value of the magnetization as a function of the spin-phonon coupling is reported in Fig. 9. The spin texture has a rectangular shape, contains 12 sites, and is 12 fold degenerate.

As for the other cases, the Lanczos results for infinite spin-phonon coupling coincide with the hard-core boson ones. As in the case of the 1/4 plateau, the spin texture con-

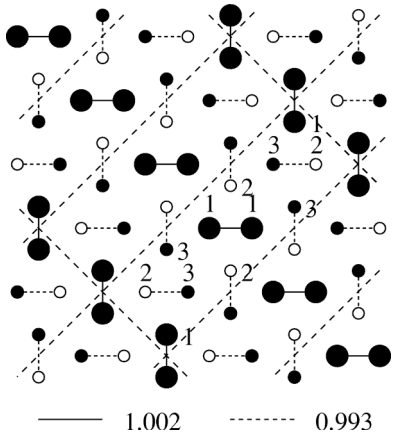

FIG. 8. Spin density profile for the 1/3 plateau. Full (empty) circles indicate sites with magnetization along (opposite to) the external field and the size of the circles is proportional to the spin amplitude. The bond lengths for $\alpha=10$ are also shown.

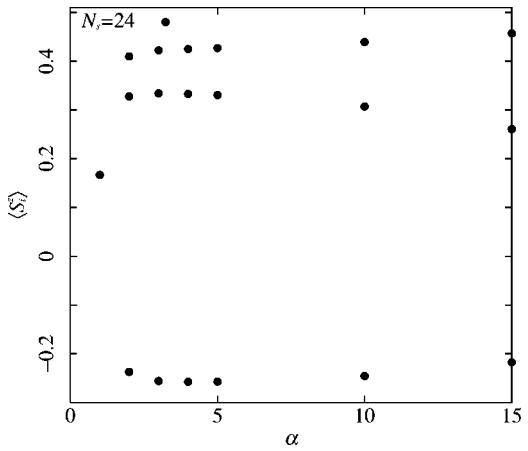

FIG. 9. Local magnetization for the three different sites for the 1/3 plateau as a function of the spin-phonon coupling α.

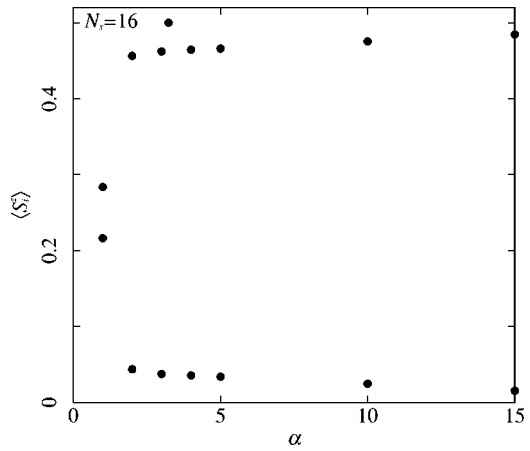

FIG. 11. Local magnetization for the two different sites for the 1/2 plateau as a function of the spin-phonon coupling α.

figuration shows diagonal ''triplet'' stripes, and this configuration is stabilized by the repulsion between strongly polarized dimers.[27–30]

D. 1/2 plateau

For completeness, we finally consider the calculations for the 1/2 plateau, by taking the 16-site cluster with $S^z_{tot}=4$. The typical spin configuration is shown in Fig. 10; here, we have only two different sites, both with positive magnetization, corresponding to two different dimers: A ''triplet,'' strongly polarized, and a ''singlet,'' with a small magnetization. Hence, we obtain a square unit cell that contains only four sites. The evolution of the two local polarizations as a function of the spin-phonon coupling is reported in Fig. 11. In this case, only the symmetry which interchange the ''triplet'' with the ''singlet'' is broken, whereas the translational symmetry is preserved. Therefore, the ground state is only twofold degenerate, corresponding to the two possible choices of the ''triplet'' position in the unit cell.

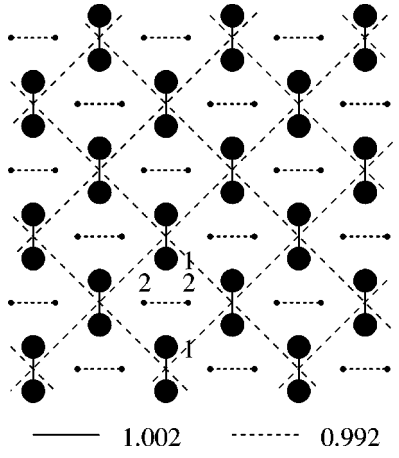

FIG. 10. Spin density profile for 1/2 plateau. Full circles indicate sites with magnetization along the external field, and the size of the circles is proportional to the spin amplitude. The bond lengths for $\alpha=10$ are also shown.

IV. COMPARISON WITH NMR EXPERIMENTS AT 1/8 PLATEAU

As stated previously, at present, due to the very high magnetic field and the low temperature needed to stabilize the plateaus, it is only possible to perform accurate NMR experiments for the 1/8 plateau, which can give useful insight into the local spin texture.[33] Therefore, in the following, we make a more detailed analysis of our numerical results for this magnetization plateau.

The Cu NMR spectra was measured at 35 mK in a field of 27.6 T, corresponding to the 1/8 plateau. The overall shape of the spectra can be well reproduced assuming at least 11 distinct sites [see Fig. 12(e)]. If we consider only the on-site dominant hyperfine coupling, the hyperfine field is written as $H_n=A_c g_c \langle S_z \rangle$, where $\langle S_z \rangle$ is the time-averaged local magnetization. The coupling constant A_c and g_c values are determined as $A_c=-23.8$ T/μ_B and $g_c=2.28$ by electron spin resonance (ESR) and NMR measurements.[14,41] Thus, the 11 sites observed in NMR indicate the existence of 11 distinct spin sites in the 1/8 plateau. Two large positive $\langle S_z \rangle$ sites (two negative hyperfine field sites) and one large negative $\langle S_z \rangle$ site (one positive hyperfine field site) can be read off from Fig. 12(e). In addition to them, several sites spread around zero.

In this plateau, two types of unit cells (square and rhomboid cells) have been proposed theoretically and so we calculated the spin textures in both unit cells as discussed in Sec. III A. In both cases, there are two large positive spin sites and one large negative spin site, which hardly depend on the shape of the unit cell. However, the distribution of the expectation values of the spin component $\langle S_z \rangle$ on the other sites is different in the two cases. In the square unit cell, the values $\langle S_z \rangle$ are concentrated around zero. On the other hand, in the rhomboid one, the expectation values spread further away from zero. These facts indicate that the results on rhomboid cell are qualitatively consistent with the results of NMR. Hyperfine fields assuming the on-site hyperfine coupling $A=A_c=-23.8$ T/μ_B are shown in Fig. 12(a) [Fig. 12(c)] for a square (rhomboid) unit cell, in the case of $\alpha=10$. Following Ref. 33, the hyperfine fields including the

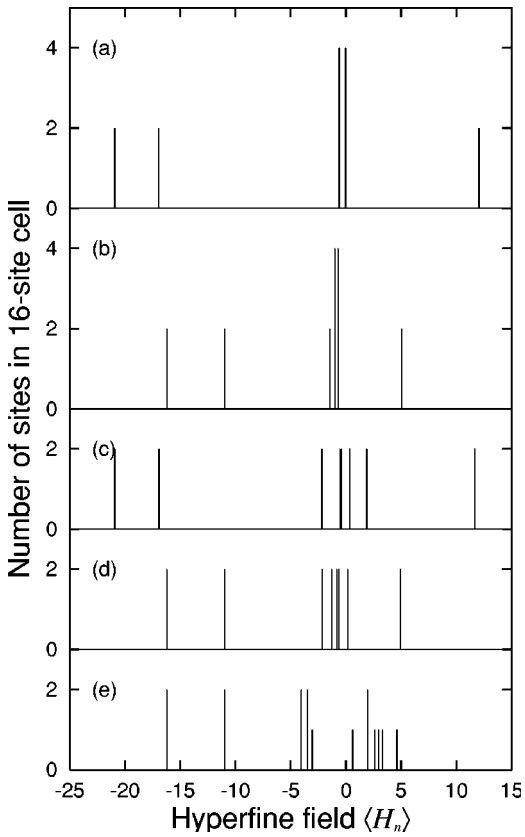

FIG. 12. Histogram of the hyperfine field $\langle H_n \rangle$. (a) The spin distribution in the square unit cell assuming only the on-site hyperfine coupling $A=A_c=-23.8\ \mathrm{T}/\mu_B$. (b) The spin distribution in the square unit cell assuming the transferred hyperfine coupling B and C. The on-site hyperfine coupling is $A=A_c-4B-C$. (c) The spin distribution in the rhomboid unit cell assuming only the on-site hyperfine coupling $A=A_c=-23.8\ \mathrm{T}/\mu_B$. (d) The spin distribution in the rhomboid unit cell assuming the transferred hyperfine couplings B and C. (e) The hyperfine field observed in NMR measurements (Ref. 33).

effects of transferred hyperfine couplings B and C (see Fig. 1) with the square (rhomboid) unit cell are also shown in Fig. 12(b) [Fig. 12(d)]. Here the parameters B and C are chosen to reproduce the two large positive sites reported in the experiments. These results support the realization of the rhomboid cell. However, it is difficult to estimate the realistic values of the transferred hyperfine couplings, and therefore the agreement of the rhomboid cell with the experiment is only indicative.

It seems that the superstructure in the rhomboid unit cell is qualitatively consistent with the state observed by NMR. There are still quantitative differences though. For example, the numbers of different spin sites are not consistent: in the rhomboid cell, there are eight different spin sites (see Fig. 3) and in the experiments at least 11 sites exist. On the other hand, there are only six different spin sites in the square unit cell. In the following we will discuss the possible effects of the inter-layer coupling and of the Dzyaloshinsky-Moriya interaction on the local spin structure and we emphasize the possible role of interlayer coupling to achieve a more quantitative agreement.

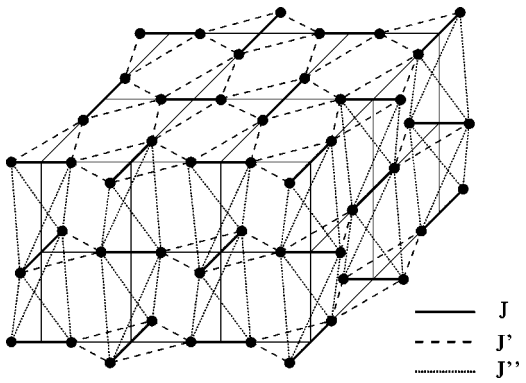

FIG. 13. The 3D orthogonal dimer model for $SrCu_2(BO_3)_2$.

A. Interlayer coupling

The three-dimensional (3D) structure of $SrCu_2(BO_3)_2$ consists of $CuBO_3$ layers, intercalated by magnetically inert Sr layers. The magnetic ions Cu^{2+} form a three-dimensional lattice structure shown in Fig. 13 and we denote the interlayer coupling by J''. However, we expect that antiferromagnetic coupling J'' is much smaller than the intra layer interactions J and J' because of the presence of the Sr layers. It is worth noting that, for small J''/J, the product of the dimer singlet, [Eq. (2)], is the ground state also for the 3D orthogonal dimer model.[42,43] In addition, in this limit, the magnitude of the triplet excitations and their dispersion relation do not depend on the interlayer interaction J''.[13] These facts further support the hypothesis that the magnetic properties of $SrCu_2(BO_3)_2$ can be very well described by the 2D orthogonal dimer model. However, the interlayer interaction J'' may affect the magnetic properties at high temperatures or under external magnetic fields. For instance, the inclusion of J'' is necessary to correctly reproduce the behavior of the magnetic susceptibility at high temperatures.[13]

Therefore, the effects of the interlayer coupling might affect the superstructures at the plateaus. Although it is not presently possible to perform an exact calculation by Lanczos diagonalization which includes a full 3D lattice, we try to combine the previous exact results with the perturbation theory based on the hard-core bosons to extract some conclusion on the possible 3D spin texture and on the possibility to obtain more than eight sites inside the unit cell. Therefore, let us begin by considering the hard-core boson picture, and, following Refs. 27–29, we calculate the interlayer interactions between triplets in two neighboring layers (which we denote by A and B planes; see Fig. 14) by using the perturbation theory in the limits $J'/J \ll 1$ and $J''/J \ll 1$. Starting from a state where one of the singlets is promoted to a triplet on each layer, up to fifth order in J'/J, the triplets are completely localized and the excitation energy is given by

$$E = 2\Delta + W_k, \tag{6}$$

where Δ is the spin gap energy for one triplet and W_k the interaction between the two triplets at distance k, see Fig. 14. Up to third order, the spin gap energy is written as $\Delta = J[1 - (J'/J)^2 - 1/2(J'/J)^3]$ and the interaction energies are given by

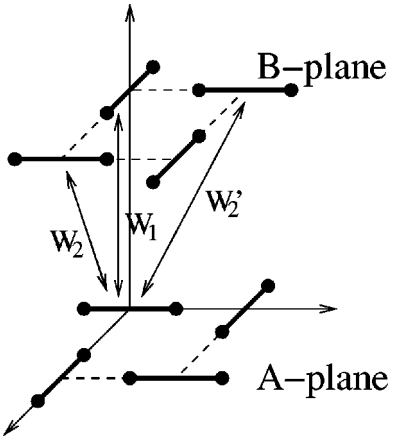

FIG. 14. Interlayer interactions between the triplet excitations. The nearest-neighbor interaction W_1, and the next-nearest-neighbor interactions W_2 and W_2' are shown.

$$\frac{W_1}{J}=\frac{J''}{J}+\left(\frac{J'}{J}\right)^2\frac{J''}{J}, \tag{7}$$

$$\frac{W_2}{J}=\frac{1}{2}\left(\frac{J'}{J}\right)^2\frac{J''}{J}, \tag{8}$$

$$\frac{W_2'}{J}=0. \tag{9}$$

The interaction energies vanish for $k>2$. Note that, similarly to what happens in the third-neighbor intralayer interaction, the interactions for $k=2$ strongly depend on the relative position of the triplets.[27–29]

In the following, we consider the case of the rhomboid unit cell, which seems to be a better condition to represent the real compound. We remind that, in this case, we have eight different sites, and therefore in each unit cell there are two equivalent sites. From the hard-core boson calculation, we can assume that the triplets on the B layer are located as far as possible from the triplets on the A layer. In this assumption, the stacking pattern for the 1/8 plateau is given in Fig. 15. When the interlayer coupling is considered, the two triplets of the cell repel each other and the two equivalent dimers in the cell of the A layer face two *different* dimers in the cell of the B layer. Therefore, because of the interlayer couplings, the two equivalent sites in a given plane can split into two different local spins: Assuming the stacking pattern of Fig. 15, we expect 14 different spin states per unit cell. In general, if we consider long-range interactions between two neighboring planes, we can obtain up to 16 different spins per unit cell. However, the splitting for the sites indicated by 1 and 2 in Fig. 15 may be negligible because the difference originates from long-range interactions.

Therefore, from this analysis, it comes out that the inclusion of the interlayer coupling can give rise to 14–16 different spin sites, which is in closer agreement with the NMR results, that indicate at least 11 different sites per unit cell. Note that in the square unit cell the number of different spin sites remains six, even including the effect of interlayer coupling J''.

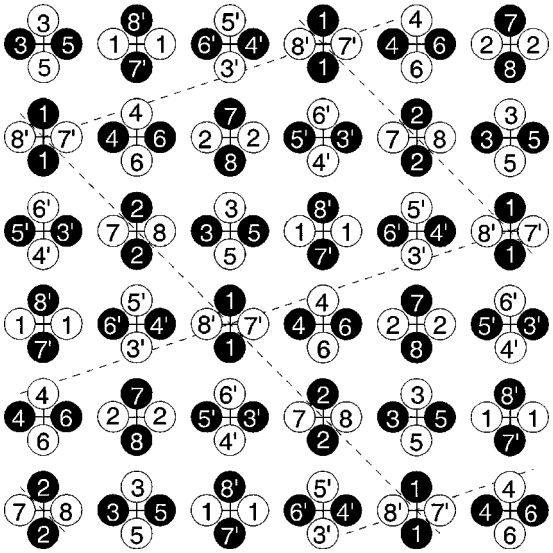

FIG. 15. A stacking pattern for two neighboring layers. Black circles are in the A plane whereas white circles are in the B plane. The numbers indicate the different spins within the unit cell (see Fig. 3); the primed numbers are used to distinguish the spins modified by the interlayer interaction.

B. Dzyaloshinsky-Moriya interaction

Finally, we consider the effect of the Dzyaloshinsky-Moriya interaction on the spin texture. Indeed, this term is relevant for $SrCu_2(BO_3)_2$: ESR and inelastic neutron scattering experiments show an anisotropic behavior of the spin gap, which depends on the direction of the external field,[14,44] and such a behavior can be explained by considering the Dzyaloshinsky-Moriya interaction.[44,45]

If, following Ref. 44, we assume in first approximation that the $CuBO_3$ layer is a mirror plane, there is a Dzyaloshinsky-Moriya term only on the J' bonds and its component is perpendicular to the plane. In that case, the Hamiltonian for the Dzyaloshinsky-Moriya coupling is

$$\mathcal{H}_{\mathrm{DM}}=D_z\sum_{(\mathrm{n.n.n.})}(S_i^xS_j^y-S_i^yS_j^x). \tag{10}$$

Note that Dzyaloshinsky-Moriya term $\mathcal{H}_{\mathrm{DM}}$ is odd under the exchange $i\leftrightarrow j$ and, therefore, we have to fix the direction from i to j for a pair i, j, as shown in Fig. 1.

Strictly speaking, in the real compound, there is a slight buckling of the $CuBO_3$ plane,[40] and so other higher components of Dzyaloshinsky-Moriya interaction can appear. However, the magnitude of this buckling is very small and therefore the higher terms might be neglected with respect to the one given by Eq. 10. In practice, we have included the Dzyaloshinsky-Moriya interaction, Eq. (10), in the original Hamiltonian [Eq. (4)] and we have performed our self-consistent Lanczos diagonalization of the 2D cluster. The results for the rhomboid cluster with $D_z/J=0.02$ and 0.04 are shown in Fig. 16 and compared with the ones for

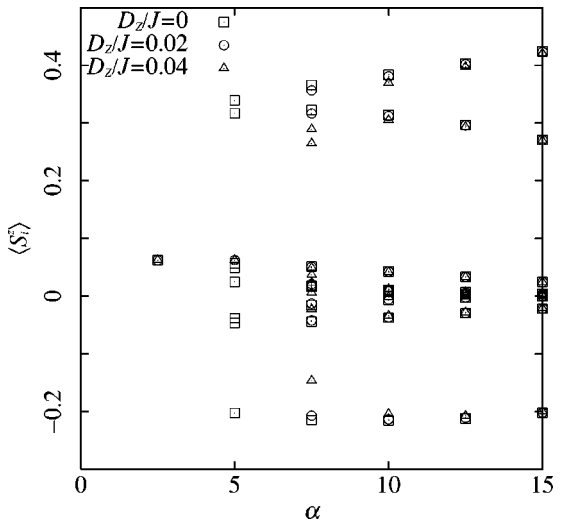

FIG. 16. Local magnetization for the eight different sites in the rhomboid unit cell for the 1/8 plateau as a function of the spin-phonon coupling for different values of the Dzyaloshinsky-Moriya interaction D_z.

$D_z=0$. The inclusion of the Dzyaloshinsky-Moriya interaction makes the uniform state more stable for small spin-phonon coupling, and the inhomogeneous state appears for a spin-phonon coupling larger that the one we obtain without this interaction. The reason for this shift is due to the fact that the Dzyaloshinsky-Moriya term favors the hopping of the triplet. On the other hand, for strong enough spin-phonon couplings, i.e., $\alpha \gtrsim 7$, the values of the local spins are only slightly modified by the Dzyaloshinsky-Moriya interaction, and the number of different spins is always equal to 8. Therefore, we can infer that the Dzyaloshinsky-Moriya interaction is not a fundamental ingredient in determining the spin texture at the magnetization plateau, and, in a first approximation, can be neglected.

V. CONCLUSION

In this paper, we have considered the effect of adiabatic phonons on the 2D orthogonal dimer model by using a self-consistent Lanczos diagonalization of small clusters. This study is directly related to the properties of $SrCu_2(BO_3)_2$, a new spin gapped material, under magnetic field. From an experimental point of view, at present, the only available informations about the magnetic texture are about the 1/8 plateau, which is stabilized for magnetic fields around 27.6 T. Our theoretical results for this plateau indicate that the spin-phonon coupling is able to stabilize two possible candidates for the local spin texture: (i) a square unit cell of 16 sites with six different values of the spins, and (ii) a rhomboid unit cell of 16 sites with eight different values of the spins. Although the energy difference between the two configurations is very small, the rhomboid cell contains a larger number of different spins and therefore it describes better the experimental finding. A closer agreement with the NMR results can be achieved by the inclusion of the interlayer coupling, that can split equivalent sites, whereas the Dzyaloshinsky-Moriya interaction does not seem to play an important role in determining the actual values of the local spins. From our calculations, it comes out that the superstructure at the 1/8 plateau is qualitatively consistent with the NMR results, but it is still an open question to make a more quantitative comparison. The main limitation of our Lanczos calculations is the presence of finite size effects. As we already emphasized previously, the finite size effects might be small because the decay of the Friedel-like oscillation of the local spins is quite fast. However, in a small cluster, the uniform state is easily stabilized, and, therefore, the spin-phonon coupling required might be bigger than the realistic value (in the thermodynamic limit). Second, as mentioned in Sec. IV, the inclusion of the transferred hyperfine couplings to neighboring spins is probably needed to reach a better agreement. Indeed we showed that the inclusion of the transferred hyperfine coupling to the nearest- and next-nearest neighbors improves the agreement between experiments and theoretical results. Moreover, it might be necessary to include also transferred hyperfine couplings from sites on neighboring layers. Assuming the stacking pattern in Fig. 15, such hyperfine couplings can induce different hyperfine fields at two equivalent sites of a given plane. Thus these hyperfine couplings enhance the effects of the interlayer couplings which we discussed in Sec. IV A. However, it is difficult to obtain reliable estimates of the transferred hyperfine couplings, and this discussion can be only indicative.

Although at present, there are no experimental results on the higher plateaus, we studied also the effects of the spin-phonon coupling for 1/4, 1/3, and 1/2 plateaus, with the hope that in the near future it will be possible to have experimental insight into the local magnetization of these plateaus (or at least some of them). Our results indicate that stripelike superstructures are realized at the 1/3 and 1/4 plateaus, whereas a structure with a square unit cell is stabilized at the 1/2 plateau. It is worth noting that all the results regarding the shape of the unit cells are consistent with the hard-core boson picture, although within this hard-core boson approximation it is not possible to obtain more than two different sites. In this respect, our Lanczos results give valuable insight into the real magnetization pattern that appears in the fascinating regions of the magnetization plateaus.

ACKNOWLEDGMENTS

It is a pleasure to thank K. Kodama, M. Takigawa, M. Horvatić, and C. Berthier for showing and explaining to us their experimental results before publication. We also thank K. Ueda, H. Kageyama, D. Poilblanc, and T. Ziman for useful discussion. This work has been supported by the Swiss National Fund.

[1] M. Azuma, Z. Hiroi, M. Takano, K. Ishida, and Y. Kitaoka, Phys. Rev. Lett. **73**, 3463 (1994).
[2] J. Darriet and L.P. Regnault, Solid State Commun. **86**, 409 (1993).
[3] For a review on $CuGeO_3$ see, e.g., J.P. Boucher and L.P. Regnault, J. Phys. I **6**, 1939 (1996).
[4] M. Isobe and Y. Ueda, J. Phys. Soc. Jpn. **65**, 3142 (1996); N. Fujiwara, H. Yasuoka, M. Isobe, Y. Ueda, and S. Maegawa, Phys. Rev. B **55**, R11 945 (1997).
[5] S. Taniguchi, T. Nishikawa, Y. Yasui, Y. Kobayashi, M. Sato, T. Nishioka, M. Kontani, and K. Sano, J. Phys. Soc. Jpn. **64**, 2758 (1995).
[6] K. Ueda, H. Kontani, M. Sigrist, and P.A. Lee, Phys. Rev. Lett. **76**, 1932 (1996).
[7] M. Troyer, H. Kontani, and K. Ueda, Phys. Rev. Lett. **76**, 3822 (1996).
[8] H. Kageyama, K. Yoshimura, R. Stern, N.V. Mushnikov, K. Onizuka, M. Kato, K. Kosuge, C.P. Slichter, T. Goto, and Y. Ueda, Phys. Rev. Lett. **82**, 3168 (1999).
[9] S. Miyahara and K. Ueda, Phys. Rev. Lett. **82**, 3701 (1999).
[10] For a review on $SrCu_2(BO_3)_2$, see S. Miyahara and K. Ueda, J. Phys.: Condens. Matter **15**, R327 (2003).
[11] B.S. Shastry and B. Sutherland, Physica B **108**, 1069 (1981).
[12] A. Koga and N. Kawakami, Phys. Rev. Lett. **84**, 4461 (2000).
[13] S. Miyahara and K. Ueda, J. Phys. Soc. Jpn. **69**, Suppl. B, 72 (2000).
[14] H. Nojiri, H. Kageyama, K. Onizuka, Y. Ueda, and M. Motokawa, J. Phys. Soc. Jpn. **68**, 2906 (1999).
[15] H. Kageyama, M. Nishi, N. Aso, K. Onizuka, T. Yosihama, K. Nukui, K. Kodama, K. Kakurai, and Y. Ueda, Phys. Rev. Lett. **84**, 5876 (2000).
[16] P. Lemmens, M. Grove, M. Fischer, G. Guntherodt, V.N. Kotov, H. Kageyama, K. Onizuka, and Y. Ueda, Phys. Rev. Lett. **85**, 2605 (2000).
[17] T. Rõõm, U. Nagel, E. Lippmaa, H. Kageyama, K. Onizuka, and Y. Ueda, Phys. Rev. B **61**, 14 342 (2000).
[18] K. Onizuka, H. Kageyama, Y. Narumi, K. Kindo, Y. Ueda, and T. Goto, J. Phys. Soc. Jpn. **69**, 1016 (2000).
[19] K. Hida, J. Phys. Soc. Jpn. **63**, 2359 (1994).
[20] K. Okamoto, Solid State Commun. **98**, 245 (1995).
[21] T. Tonegawa, T. Nakao, and M. Kaburagi, J. Phys. Soc. Jpn. **65**, 3317 (1996).
[22] Y. Narumi, M. Hagiwara, R. Sato, K. Kindo, H. Nakano, and M. Takahashi, Physica B **246-247**, 509 (1998).
[23] M. Oshikawa, M. Yamanaka, and I. Affleck, Phys. Rev. Lett. **78**, 1984 (1997).
[24] T. Tonegawa, T. Nishida, and M. Kaburagi, Physica B **246-247**, 368 (1998).
[25] K. Totsuka, Phys. Rev. B **57**, 3454 (1998).
[26] M. Oshikawa, Phys. Rev. Lett. **84**, 1535 (2000).
[27] T. Momoi and K. Totsuka, Phys. Rev. B **61**, 3231 (2000).
[28] T. Momoi and K. Totsuka, Phys. Rev. B **62**, 15 067 (2000).
[29] S. Miyahara and K. Ueda, Phys. Rev. B **61**, 3417 (2000).
[30] Y. Fukumoto and A. Oguchi, J. Phys. Soc. Jpn. **69**, 1286 (2000).
[31] Y. Fukumoto, J. Phys. Soc. Jpn. **70**, 1397 (2001).
[32] G. Misguich, Th. Jolicoeur, and S.M. Girvin, Phys. Rev. Lett. **87**, 097203 (2001).
[33] K. Kodama, M. Takigawa, M. Horvatić, C. Berthier, H. Kageyama, Y. Ueda, S. Miyahara, F. Becca, and F. Mila, Science **298**, 395 (2002).
[34] S. Zherlitsyn, S. Schmidt, B. Wolf, H. Schwenk, B. Lüthi, H. Kageyama, K. Onizuka, Y. Ueda, and K. Ueda, Phys. Rev. B **62**, 6097 (2000).
[35] B. Wolf, S. Zherlitsyn, S. Schmidt, B. Lüthi, H. Kageyama, and Y. Ueda, Phys. Rev. Lett. **86**, 4847 (2001).
[36] W.A. Harrison, *Electronic Structure and the Properties of Solids* (Dover, New York, 1980).
[37] J. Riera and D. Poilblanc, Phys. Rev. B **59**, 2667 (1999); *ibid.* **62**, 16 243 (2000).
[38] F. Becca and F. Mila, Phys. Rev. Lett. **89**, 037204 (2002).
[39] See for instance: F. Becca, F. Mila, and D. Poilblanc, cond-mat/0209278 (unpublished).
[40] K. Sparta, G.J. Redhammer, P. Roussel, G. Heger, G. Roth, P. Lemmens, A. Ionescu, M. Grove, G. Güntherodt, F. Hüning, H. Lueken, H. Kageyama, K. Onizuka, and Y. Ueda, Eur. Phys. J. B **19**, 507 (2001).
[41] K. Kodama, J. Yamazaki, M. Takigawa, H. Kageyama, K. Onizuka, and Y. Ueda, J. Phys.: Condens. Matter **14**, 319 (2002).
[42] K. Ueda and S. Miyahara, J. Phys.: Condens. Matter **11**, L175 (1999).
[43] A. Koga, J. Phys.: Condens. Matter **69**, 3509 (2000).
[44] O. Cépas, K. Kakurai, L.P. Regnault, T. Ziman, J.P. Boucher, N. Aso, M. Nishi, H. Kageyama, and Y. Ueda, Phys. Rev. Lett. **87**, 167205 (2001).
[45] S. Miyahara and K. Ueda, J. Phys. Soc. Jpn. **70**, Suppl. B, 180 (2001).